

2017

## Effect of Post-Annealing Treatment on Mechanical Properties of ZnO Thin Films

Vipul Bhardwaj

*Department of Metallurgical and Materials Engineering, Indian Institute of Technology Roorkee, Roorkee-247667, India, mondayalive@gmail.com*

Rajib Chowdhury

*Department of Civil Engineering, Indian Institute of Technology Roorkee, Roorkee-247667, India, rajibfce@iitr.ernet.in*

R. Jayaganthan

*Department of Metallurgical and Materials Engineering, Indian Institute of Technology Roorkee, Roorkee-247667, India \ Department of Engineering Design, Indian Institute of Technology Madras, Chennai-600036, India, metarj@iitm.ac.in*

Follow this and additional works at: <https://digitalcommons.aaru.edu.fo/ijtfst>

---

### Recommended Citation

Bhardwaj, Vipul; Chowdhury, Rajib; and Jayaganthan, R. (2017) "Effect of Post-Annealing Treatment on Mechanical Properties of ZnO Thin Films," *International Journal of Thin Film Science and Technology*. Vol. 6 : Iss. 1 , Article 5.

Available at: <https://digitalcommons.aaru.edu.fo/ijtfst/vol6/iss1/5>

This Article is brought to you for free and open access by Arab Journals Platform. It has been accepted for inclusion in International Journal of Thin Film Science and Technology by an authorized editor. The journal is hosted on [Digital Commons](#), an Elsevier platform. For more information, please contact [rakan@aarj.edu.fo](mailto:rakan@aarj.edu.fo), [marah@aarj.edu.fo](mailto:marah@aarj.edu.fo), [u.murad@aarj.edu.fo](mailto:u.murad@aarj.edu.fo).

# Effect of Post-Annealing Treatment on Mechanical Properties of ZnO Thin Films

Vipul Bhardwaj<sup>1</sup>, Rajib Chowdhury<sup>2</sup> and R. Jayaganthan<sup>1,3,\*</sup>

<sup>1</sup>Department of Metallurgical and Materials Engineering, Indian Institute of Technology Roorkee, Roorkee-247667, India

<sup>2</sup>Department of Civil Engineering, Indian Institute of Technology Roorkee, Roorkee-247667, India

<sup>3</sup>Department of Engineering Design, Indian Institute of Technology Madras, Chennai-600036, India

Received: 21 Feb. 2016, Revised: 22 Dec. 2016, Accepted: 24 Dec. 2016.

Published online: 1 Jan. 2017.

**Abstract:** The present work was focused to study nanomechanical properties of ZnO thin films deposited on different substrates (Corning Glass and Fused Quartz) using DC-sputtering. The crystallinity and microstructure are correlated with process conditions and post annealing treatment in NH<sub>3</sub> environment, which in turn affects the mechanical performance. The structural growth accompanied a change in crystalline nature and microstructure as the substrate is altered from corning glass substrate to fused quartz at similar synthesis conditions. The post deposition annealed ZnO thin films demonstrated agglomerated particles with no clear grain boundaries having nano-cracks present in the morphology, which is attributed as NH<sub>3</sub> effect on microstructure. The mechanical properties such as hardness (6.89-7.76 GPa), Young's modulus (94.9-124.6 GPa), and coefficient of friction (~1.0-3.0) of ZnO thin films were measured using three sided pyramidal Berkovich nanoindentation. Load-unload segment of indentation curve of thin films which is measured at continuous loading revealed no event of discontinuity ( $\geq 2$  nm) during loading/unloading, indicating no fracture or delamination during indentation. The critical load of ZnO thin films failure was analysed using scratch testing ramp loading and the value of critical load was found around 535.6  $\mu$ N to 668.4  $\mu$ N.

**Keywords:** Thin Films; Nanoindentation; Microstructure; Adhesive Strength.

## 1 Introduction

Zinc oxide as thin films has achieved an enormous interests due to its multi-functionality and applicability in various applications [1]. The n-type inherent conductivity, wide band gap ( $E_g \sim 3.3$ eV), large excitonic energy ( $\sim 60$  meV) and c/a ratio  $\sim 1.6018$  of ZnO enable its application as antireflective coatings, transparent electrode in solar cells and grating in optoelectronics devices [1, 2]. Epitaxial growth of the ZnO thin films paves a way to superior functional properties like luminescence properties for light emitting diode [3]. Moreover, a buffer layer is incorporated as an intermediate layer between ZnO thin films and substrate to ensure lattice matching and chemical stability for ZnO thin films [4].

Recently, a lot of focus is shown for exploiting ZnO thin films in sensing applications e.g. for CO [5], ethanol vapours [6], hydrogen, liquid petroleum gas [7], SF<sub>6</sub>, C<sub>4</sub>H<sub>10</sub>, gasoline, C<sub>2</sub>H<sub>5</sub>OH [8] and NO<sub>2</sub> [9] etc. NH<sub>3</sub> is a hazardous and toxic gas, which is regularly used in many industries such as manufacturing of plastics and pesticides. The detection of NH<sub>3</sub> and using it in a controlled way is of utmost importance in chemical industries.

Hence, ZnO thin films can be employed for sensing NH<sub>3</sub> [10, 11] due to its remarkable properties as higher photoelectric response with higher electron mobility and semi-conducting nature [12].

The sensing properties of ZnO films depend on change in response properties with the microscopic interaction of foreign environment e.g. NH<sub>3</sub> etc., that interaction leads to change in microstructure as well. As far as thin films are concerned, the residual stresses and microstructure evolution such as size-shape and distribution of grains has a huge impact on underlying mechanical response. In the thin films, a huge proportion of particles resides at interface which give rise to competitive growth in particular texture and microstructure under the influence of surface energy [13].

In thin films, for non-homogeneous growth or bi-modal microstructure, distinct zones have been formed and showed a variation in mechanical properties such as hardness and Young's modulus depending upon the growth to processing conditions [14]. The porosity in the thin films can emerge as a result of shadowing effect during growth

\*Corresponding author E-mail: [rjayafmt@iitr.ernet.in](mailto:rjayafmt@iitr.ernet.in), [metarj@iitm.ac.in](mailto:metarj@iitm.ac.in)

and it can degrade the mechanical properties [15]. The crack can be induced in the coatings during plastic deformation in indentation, crack morphology observed to be dependent on grain morphology specifically grain boundaries as well as cohesive energy between grain boundary [16].

The processing-microstructure and property are interrelated with each other. In this context, the crystallinity, microstructure and defect concentrations can be varied effectively by varying growth condition in synthesis technique [17]. The sputtering paves a way to get highly crystalline growth of thin films with better adhesive strength. There are several sputtering parameters such as substrate temperature, working pressure, Ar/O<sub>2</sub> ratio, and substrate-target distance, which can be varied during synthesis. The microstructure can be manipulated at different tilt angle of substrate with respect to the target [18]. However, high quality thin films depend on growth mechanism, which is also connected with substrate properties. The corning glass and fused quartz substrate are cheap and of commercial interests in various potential application[19].

Recently, the surface specific analysis of elastic-plastic response such as hardness, Young's modulus as well as adhesion between the thin films and substrate has been made using Nano-indentation technique, which is considered to be more reliable and accurate at nano-level as compared to conventional measurements. Nano- scratch test of thin films enables to obtain failure modes (spalling, chipping, buckling etc.) and get critical load for thin film failure as well as coefficient of friction [20, 21]. For thin films deposited on substrates, there is a finite probability of overestimated or underestimated mechanical response of thin films dominated by substrate effect. However, a general approach to overcome substrate effect can be adopted in which the indentation depth is constrained below 20% of thickness of films when the film thickness is less than 1  $\mu\text{m}$  [22]. The reliability and reuse of ZnO thin films based devices especially for NH<sub>3</sub> sensing application depends upon its structural integrity affected by its strength, which is sensitive to aggressive environment. Therefore, it is essential to investigate the mechanical durability of thin films after exposure of NH<sub>3</sub> radiation.

The cost-effectiveness of manufacturing of ZnO thin films as a sensing purpose depends upon whether it can be reused multiple times with same mechanical strength. The present study is focused to study the mechanical response of films after post annealing treatment in ammonia environment on different substrates (corning glass and fused quartz). The ZnO films upon post-annealing treatment are characterized by XRD, AFM, SEM and Nanoindentation technique. The observed mechanical properties such as critical load for failure, hardness, and scratch resistance of ZnO thin films are correlated with micro structural morphologies influenced by NH<sub>3</sub> environment.

## 2 Experimental

ZnO thin films were deposited simultaneously on corning glass substrate and fused quartz substrate at different substrate temperature (100<sup>o</sup> C & 200<sup>o</sup> C) using DC-sputtering. Both substrates were put together on substrate holder and deposited thin films in a single run keeping other sputtering parameters constant except substrate temperature. Before deposition, substrates were cleaned ultrasonically in acetone for at least 15 minutes to remove any surface contamination layer to achieve homogenous growth of thin films. Circular ZnO disc was used as target materials, which was prepared as mentioned in our previous work [23].

The sputtering chamber was evacuated to  $2 \times 10^{-5}$  Torr to eliminate the residual gases in the chamber. Thereafter, high purity gas Ar:O<sub>2</sub> (20:5 sccm) was introduced in to the chamber. Other sputtering parameters; working pressure Ar/O<sub>2</sub>, sputtering power were 10mTorr, 50W, respectively maintained at same level throughout the process. The pre-sputtering was carried out for 10 minutes to eliminate surface contamination of the target. The substrate temperature was fixed at 100<sup>o</sup>C and 200<sup>o</sup>C, subsequently.

### 2.1 Post deposition annealing in NH<sub>3</sub>

After deposition, ZnO thin films were annealed in NH<sub>3</sub> atmosphere at 2 mbar chamber pressure for 1 hour duration. The chamber was evacuated to vacuum (10<sup>-2</sup> torr) and during annealing of ZnO thin films, pure NH<sub>3</sub> (99.99%) was introduced in the chamber when the required temperature is achieved. The annealing temperature is maintained same as the substrate temperature during the deposition process, 100<sup>o</sup> C and 200<sup>o</sup> C, respectively. The schematic of whole process presented in Fig.1. The ZnO thin films deposited on corning glass substrate at 100<sup>o</sup> C, and 200<sup>o</sup> C are referred as Sample-C1 and Sample-C2, while ZnO thin film deposited at 100<sup>o</sup>C and 200<sup>o</sup>C on fused quartz substrate are termed as Sample-Q1 and Sample-Q2, respectively.

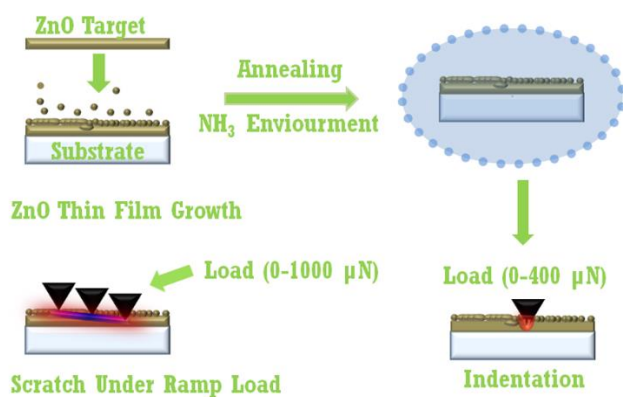


**Figure 1-** Schematic diagram of deposition and annealing process.

Structural properties of ZnO thin films after annealing were characterized by room temperature X-ray diffraction (XRD) measurements performed with Cu-K $\alpha$  radiation using X-ray diffractometer (Bruker AXS, D8 Advance). Diffractograms recorded data in the angular range of 25-70 $^{\circ}$ . The structural analysis by XRD measurements is based upon coherently diffracting domains in the materials, which provide information as full width at half maximum (FWHM) of diffraction peaks along their respective positions. Scherer's approach to get the grain size given in Eq. (1) depends on FWHM (in radians), 'K' is shape factor,  $\lambda$  is the X-ray wavelength and ' $\theta$ ' is the Bragg angle. However, the broadening of peaks depends on several other factors in thin films, as interpretation of the peak broadening is not straightforward [23].

$$D = \frac{k\lambda}{\beta \cos\theta} \quad (1)$$

## 2.2 Nanoindentation

Nanoindentation measurements on ZnO thin films were performed using Berkovich tip with a radius of ~100 nm. Hardness, Young's modulus, and coefficient of friction of ZnO thin films were obtained by Hysitron TI-950 Nanoindenter (Triboscan. software) having the load resolution < 1nN, displacement resolution < 0.04 nm. The loading rate is maintained at the constant value 50  $\mu$ N/s; and the holding time of 2 seconds at maximum load. The factors like noise, thermal drift, indenter tip geometry, pile up or sinking in effect, indentation size effect etc. can affect the measurement of mechanical properties. Indentation is performed in a closed chamber equipped with vibration isolation unit. Before performing indentation, the machine compliance and tip area function of indenter tip were calibrated on standard fused silica sample. The hardness and Young's modulus of the thin films were calculated from load-unload curve using the Oliver and Pharr method [20]. However, Oliver and Pharr developed a method for testing the monolithic materials but it is adopted now as a standard method for indentation of thin films also [24].

The scratch tests were performed on ZnO thin films using the Berkovich tip by applying a progressively increasing normal load 0-1000  $\mu$ N with the loading rate of 33.34  $\mu$ N/s for 30 seconds (Scratch time; 8s-38s). The objective of progressive normal load applied during scratch is to find the critical normal load at which films is detached. The scratch length was 10  $\mu$ m (Scratch time; 8s-38s) in each test. The thickness and morphology of thin films are determined by using FE-SEM (Carl Zeiss, Ultra Plus). The RMS roughness and surface topography of ZnO thin films were characterized by using the Atomic force microscopy (NT-MDT Ntegra) with integrated optical view system.

## 3 Result and discussion

XRD pattern of DC-sputtered and post deposition annealed ZnO thin films is shown in Fig. 2. Post annealing treatment

is used to alter the properties of ZnO thin films [25]. XRD patterns of ZnO thin films show a crystalline growth of thin

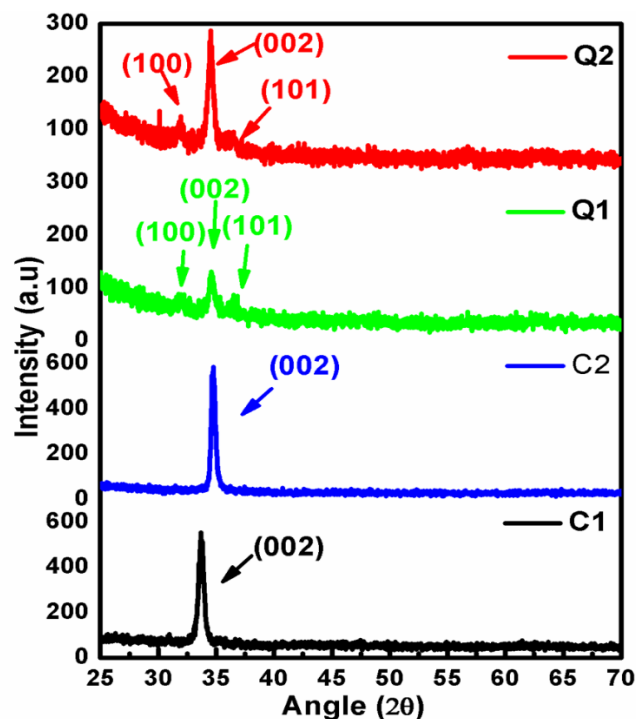


Figure 2- XRD pattern of ZnO thin film.

films with predominantly (002) crystal plane. However, presence of low peak intensity of (101) and (100) crystal planes originated in ZnO thin films is observed on fused quartz. ZnO thin films deposited on corning glass substrate show a single diffraction peak and textured in (002) plane. XRD pattern revealed that growth of ZnO thin films along peak at  $2\theta \sim 33.68^{\circ}$  range corresponds to (002) plane, which has hexagonal crystal structure (JCPDS card 89-1397). No diffraction peak related to 'N' or its crystalline phases is observed within the detection limit of XRD measurement of ZnO thin films. It is revealed from XRD pattern that ZnO thin films on corning glass show high XRD peak intensity with exhibiting better crystallinity in c-axis orientation as compared to the films on fused quartz substrate. However, the crystallinity improved at elevated temperature correlated with higher thermal energy, reflects high adatoms mobility to achieve better crystallization [26]. The interaction of ad-atoms on the substrate is influenced in such a way that they tend to grow in a plane to minimum surface energy by diffusion. Drift model suggested that evolution of crystal plane is more favorable to grow with fastest rate of growth [27]. Different substrate induce a different final state of stress as a combination of different lattice mismatch effect, thermal expansion mismatch effect and interfacial stress which overall affect the growth of thin films [28]. The broadening of the peaks is attributed to the coherent domain size of crystallites present and stress in ZnO films. The Bragg's angle position and (002) XRD peaks of annealed ZnO thin films have shifted towards

higher  $2\theta$  side at higher substrate temperature for corning glass substrate, while just reverse is observed for ZnO thin films deposited on fused quartz. Concomitantly, (002) diffraction plane emerged with

**Table-1:** Properties of ZnO thin films.

ZnO thin film deposited on substrate	Sample Name	Position of peak ( $2\theta$ ) (002)	d-spacing ( $\text{\AA}$ )	Crystallite Size (nm)	Thickness (nm)
Corning glass (100°C)	C1	33.68	2.65890	17.5	~230
Corning glass (200°C)	C2	34.7235	2.58133	22.1	~250
Fused Quartz (100°C)	Q1	34.5911	2.59097	15.7	~230
Fused Quartz (200°C)	Q2	34.4904	2.59831	17.4	~250

higher intensity and influenced the grain growth process at elevated substrate temperature, where the coherent grain size from 15.7 nm to 22.1 nm is observed and given in Table 1. The lattice spacing ( $d_{002}$ ) has decreased to 2.5813  $\text{\AA}$  close to reference set ( $d_{\text{ref}} = 2.6065$ , JCPDS card 89-1397) of crystal structure of ZnO. Several properties of ZnO thin films are driven by its crystalline phase and crystallinity. However, the microstructure affects its type of growth, density and roughness, which in turn affect mechanical reliability of thin films. By changing the processing conditions, it could lead to a slight change in crystallinity and microstructure, which influence mechanical properties of the films significantly

### 3.1 Indentation and Scratch behavior of post-deposition annealed ZnO thin films

The mechanical performance of thin films is correlated with type of bonding (ionic or covalent), cohesive energy, fracture and deformation characteristics. The indenter approached downwards to make adequate plastic contact with surface of ZnO thin films, the interaction of indenter tip and material response at a particular load is estimated using loading-displacement curve. Initially, thin films tend to deform elastically until complex stress (internal as well as applied by indenter) is greater than film yield strength and subsequently the plastic deformation takes place. The deformation characteristics during loading-unloading of the ZnO thin films at different deposition conditions are shown in Fig. 3. The load-displacement curve are recorded during indentation are continuous and consistent without any major discontinuity ( $\geq 2$  nm) during either loading or unloading of indenter. So, no fracture or delamination event of films is observed, neither pop-in nor pop-out during

loading or unloading segment in indentation process. However, the presence of saw type serrations in loading curve implies the effect of shear band nucleation and propagation, which is generally loading rate dependent [29].

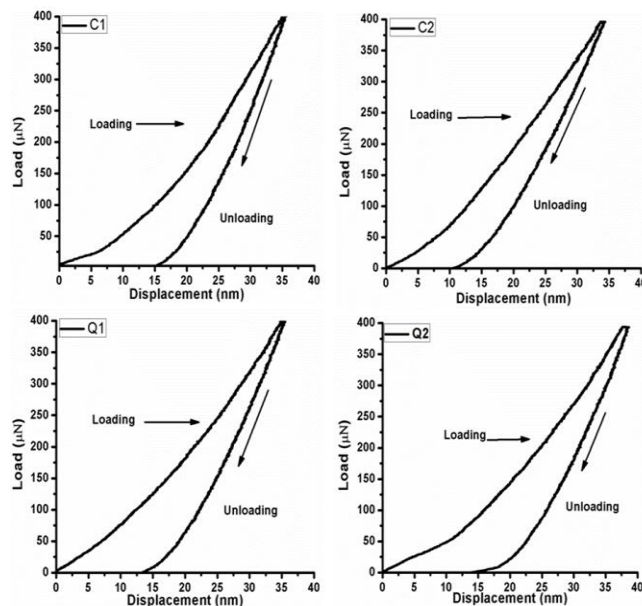


**Figure 3-** The Loading-Unloading Curves of ZnO thin films.

For the reliable results, at least 10 indents were taken on each sample having the spacing of 20  $\mu\text{m}$  to avoid the effect of pre-indent morphology. The hardness and Young's modulus are provided after multi-curve analysis and averaging with standard deviation as shown in Table 2. ZnO in bulk state shows anisotropic mechanical properties, a-plane & c-plane ZnO show hardness and Young's modulus of  $2.2 \pm 0.2$  GPa,  $4.8 \pm 0.2$  GPa,  $163 \pm 6$  GPa and  $143 \pm 6$  GPa, respectively [30]. The ZnO thin films show hardness value of roughly 6-10 GPa depending upon their crystallinity and microstructure[30, 31]. However, in the present work, variation in hardness is found to be 6.89 to 7.76 GPa and almost similar for ZnO thin films deposited on fused quartz as well as corning glass. It reveals that substrate effect is less significant up to the indentation penetration depth up to 20 percent to the total thickness of ZnO thin films. It is noteworthy that although the variation in hardness is slight but standard deviation is reduced at higher temperature, indicating the uniformity in hardness throughout the films. It is well known that wear is predominately dependent on hardness of materials, however, recent study revealed that the wear behavior is also predicted by hardness to Young's modulus ratio, 'plasticity index' as compared to hardness only [32]. The high H/E index indicates better wear resistance properties. In the present case of ZnO thin films, H/E ratio is given in Table 2.

For any practical application of thin films, a threshold level of adhesive strength should be achieved for the successful operation of devices. The scratch under ramp loading induces an increasing amount of normal mechanical force

to detach the coating termed as critical load of coating shown in the Fig. 4 [21].

**Table-2:** Mechanical parameter and roughness of films

S.No	ZnO thin film deposited on substrate	Sample Name	Hardness (GPa)	Young's Modulus (GPa)	Critical Load ( $\mu\text{N}$ )	H/E	RMS Roughness (nm)
1	Corning glass (100°C)	C1	7.34 $\pm$ 1.02	119.07 $\pm$ 12.37	540.6	.061	4.7
2	Corning glass (200°C)	C2	6.9 $\pm$ 0.27	94.95 $\pm$ 5.02	661.3	.072	2.72
3	Fused Quartz (100°C)	Q1	6.89 $\pm$ 0.62	95.98 $\pm$ 6.47	668.4	.072	23.5
4	Fused Quartz (200°C)	Q2	7.76 $\pm$ 0.27	124.63 $\pm$ 10.97	535.6	.062	7.3

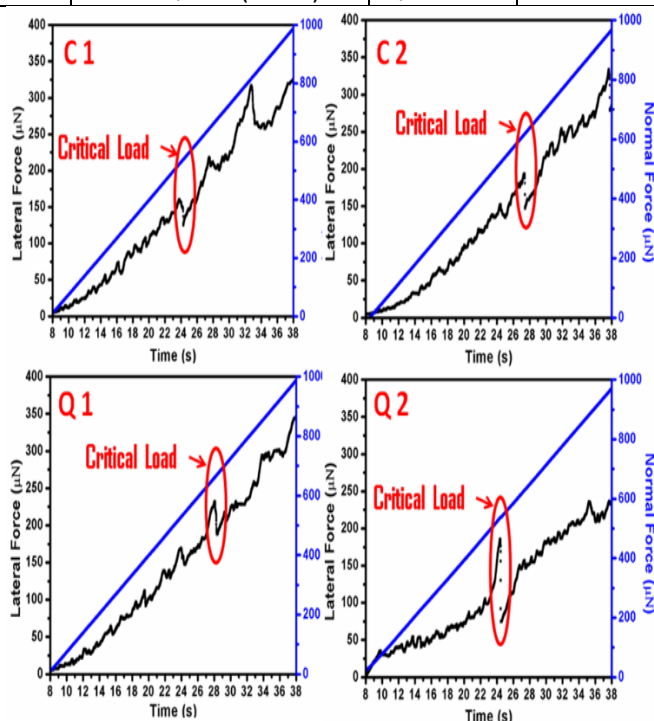


**Figure 4-** The Lateral force and respective normal force of ZnO thin films.

During the scratch testing, indenter tip and film surface was in relative motion and experience a tribological response in terms of friction depend upon underlying film materials and contact mechanics of indenter. The coating-substrate correlated properties are influenced by interfacial stress, coating thickness and coefficient of friction, which influences the critical load. The complex stress state developed during scratch depends on normal load, indenter dynamics as well as internal stress state in the coating [33]. The adhesion of the thin films itself depends upon of adhesion between substrate to film as well as cohesive nature of film materials. The microstructure and crystallinity correlated each other to influence adhesive strength [34]. If distribution of the oxygen throughout the lattice in ZnO is changed, the bonding nature of ZnO is altered as well as the ionic character is changed

substantially, which can lead to distortion of bonds [35]. The critical load for the post deposition annealed ZnO film failure is varied from 535.6  $\mu\text{N}$  to 668.4  $\mu\text{N}$ , however in previous reported literature on ZnO thin film without  $\text{NH}_3$  radiation have higher adhesive strength indicating that in present work films become more prone to fracture and delamination after  $\text{NH}_3$  exposure [23, 36]. The cohesive nature of the films is reduced after  $\text{NH}_3$  exposure. It is noteworthy that maximum load at indentation is 400  $\mu\text{N}$  at which there is no significant fracture or delamination; however during scratch ZnO thin films show poor adherence and critical load for coating failure varied from 535.6  $\mu\text{N}$  to 668.4  $\mu\text{N}$ . The difference between indentation load and critical load is not much; this is attributed as the effect of frictional stored energy by lateral forces. So, indentation load ought to be higher to invoke delamination as compared to frictional forces [37].

The initial part of the scratch is rather dependent on the surface asperities and surface layer behavior shown in the Fig. 5. The coefficient of friction is the ratio between lateral forces and normal forces, both forces vary too much extent during initial phase of scratch due to lack of appropriate contact of tip with film surface.

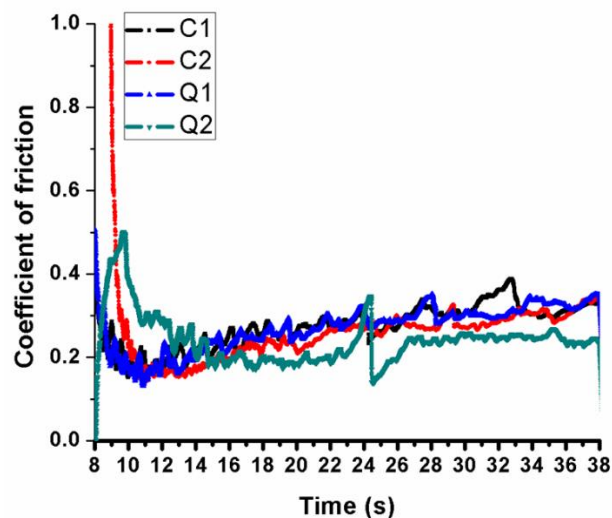


**Figure 5-** Coefficient of friction of ZnO thin films.

The plastic sliding of indenter takes place, when the higher normal load applied and indenter moves down to deeper normal penetration depth, the plastic-friction effect becomes well pronounced. Afterwards, the coefficient of friction is oscillating within steady state during scratch until any discontinuity occurred. The oscillation is considered due to the stick slip motion of the indenter. However, the stick-slip mechanism including stick-slip amplitude and stick-slip frequency relies on velocity of tip sliding, rough surface and phase transitions and fracture event primarily [38]. The average value of coefficient of friction lies between 0.1 to 0.3 shown in Fig. 5.

### 3.2 Surface Morphology and Roughness

$\text{NH}_3$  gas, which is considered as reducing gas introduced into chamber at different temperature interact with surface oxygen. Generally, when ZnO thin films are exposed to external environment, oxygen is adsorbed to the film surface. The interaction of  $\text{NH}_3$  with adsorbed oxygen took place [12]. During the treatment of ammonia gas, nitrogen atom may incorporate into ZnO microstructure, this lead to change in chemical environment around Zn [39].

This affect the bonding state between Zn and O, the overall effect of ammonia treatment induce a change in microstructure. The nano-tribological performance of coatings depends upon grain to grain distribution and asperities to asperities in the coated surface. Shear forces and fracture are responsible for the nucleation and propagation of the crack. However, critical load of failure also depends upon the pre-existing defect, voids or cracks along with other film properties. Sometime, the fracture load can vary a factor of 10 depending upon the coating thickness and other properties [40].

The micro structural features of ZnO thin films are characterized through FE-SEM and AFM. The surface morphology of ZnO thin films on corning glass/fused quartz is shown in Fig. 6. It is clear from this Fig. 6 that ZnO thin films show non-uniform distribution of grains, which is agglomerated to specific areas throughout morphology without clear grain boundaries. At low substrate temperature of deposition, the agglomerates of grains are more pronounced in the morphology. The presence of voids and nano-crack at the surface of film indicate loss of adhesive strength in the film, eventually, these nano-cracks extend to cause delamination of films under local stress applied by indenter. As ZnO thin films deposited on both corning glass and fused quartz simultaneously, the thickness of the films was analysed after fracturing the films through cross-sectional analysis as given in Table 1.

The AFM measurements involved finding presence of domes and crater on the films surface shown in the Fig. 7 through tapping mode. Roughness is one of the primary parameters that can affect mechanical properties of films, as all surfaces (tip and film surface) have a finite value of

roughness when the indenter comes in contact with coating. It initially interacts first the asperities, as the indenter approaches to surface by deforming the asperities, the contact mechanics and average stress distribution changes. The friction coefficient depends on the statistical distribution of contact between different asperities. So, initially the major scratch behavior is contributed by the roughness, frictional forces show complex nature in this segment. However, apart from initial condition, the frictional forces is the sum of normal forces as well as tangential forces [41].

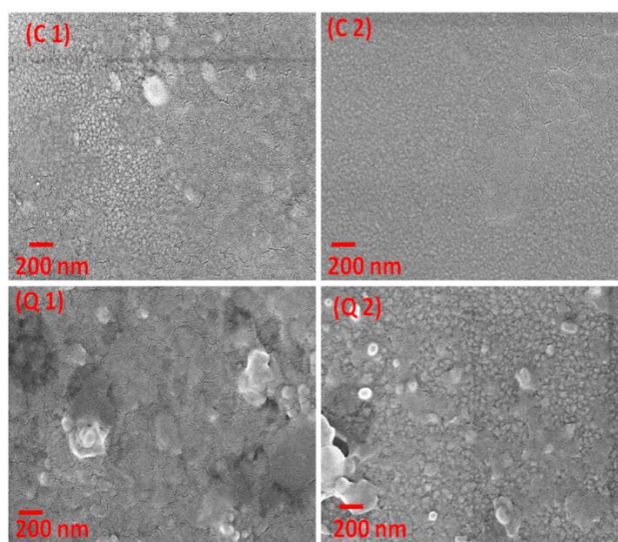


Figure 6- FESEM micrographs of ZnO thin films.

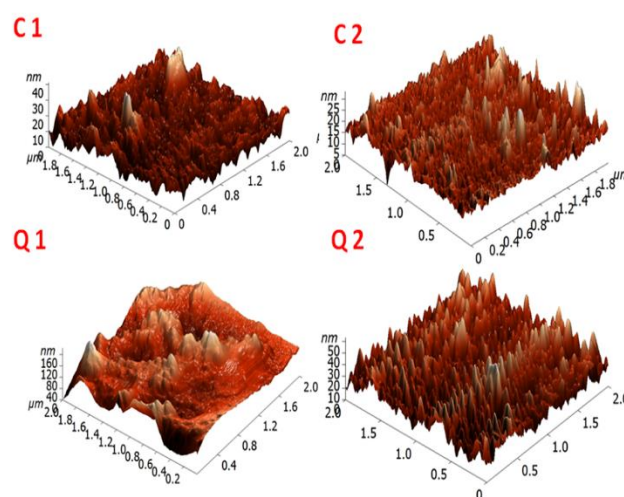


Figure 7- AFM micrographs of ZnO thin films.

## 4 Conclusion

DC sputtering was used to deposit crystalline ZnO thin films on corning glass and fused quartz substrate at same synthesis condition followed by post annealing in pure  $\text{NH}_3$ . The mechanical properties of films are investigated by continuous indentation cycle and scratch testing under

ramp load. The following conclusions are made based on the present work.

- The ZnO thin films were successfully deposited using DC-sputtering which is predominately c-axis oriented and grain size varied from 15.7 nm to 22.1 nm, it increases at elevated temperature with better crystallinity. The crystalline growth of ZnO thin films has varied and shown a marked influence underlying substrate.
- The morphology and surface topography revealed that distribution of grains at surface has varied with synthesis conditions. The morphology of ZnO thin films having voids and nano-cracks distributed to specific areas in the morphology.
- The RMS roughness of ZnO thin films has decreased (2.7 nm at corning glass, 7.3 nm at fused quartz) with denser and uniform grains at high substrate temperature.
- There is no observation of major sudden discontinuity neither in loading segment nor in unloading segment during the indentation process. It reveals that films can withstand at the maximum load of 400  $\mu\text{N}$  without fracture or delamination.
- The critical load of failure of post deposition annealed ZnO thin films is varied between around 535.6  $\mu\text{N}$  to 668.4  $\mu\text{N}$  and follows the H/E ratio.

## References

- [1] Ü. Özgür, Y.I. Alivov, C. Liu, A. Teke, M. Reshchikov, S. Doğan, V. Avrutin, S.-J. Cho, H. Morkoc, A comprehensive review of ZnO materials and devices, *Journal of Applied Physics*, 98 (2005) 041301.
- [2] M. Sucheck, S. Christoulakis, K. Moschovis, N. Katsarakis, G. Kiriakidis, ZnO transparent thin films for gas sensor applications, *Thin Solid Films*, 515 (2006) 551-554.
- [3] S. Kyun Lee, J. Yeog Son, Epitaxial growth of thin films and nanodots of ZnO on Si(111) by pulsed laser deposition, *Applied Physics Letters*, 100 (2012) 132109.
- [4] W. Guo, M.B. Katz, C.T. Nelson, T. Heeg, D.G. Schlom, B. Liu, Y. Che, X.Q. Pan, Epitaxial ZnO films on (111) Si substrates with Sc<sub>2</sub>O<sub>3</sub> buffer layers, *Applied Physics Letters*, 94 (2009) 122107.
- [5] J. Chang, H. Kuo, I. Leu, M. Hon, The effects of thickness and operation temperature on ZnO: Al thin film CO gas sensor, *Sensors and actuators B: Chemical*, 84 (2002) 258-264.
- [6] M. Miki-Yoshida, J. Morales, J. Solis, Influence of Al, In, Cu, Fe and Sn dopants on the response of thin film ZnO gas sensor to ethanol vapour, *Thin Solid Films*, 373 (2000) 137-140.
- [7] P. Mitra, A.P. Chatterjee, H.S. Maiti, ZnO thin film sensor, *Materials Letters*, 35 (1998) 33-38.
- [8] J. Xu, Q. Pan, Y.a. Shun, Z. Tian, Grain size control and gas sensing properties of ZnO gas sensor, *Sensors and actuators B: Chemical*, 66 (2000) 277-279.
- [9] S.T. Shishiyanu, T.S. Shishiyanu, O.I. Lupan, Sensing characteristics of tin-doped ZnO thin films as NO<sub>2</sub> gas sensor, *Sensors and actuators B: Chemical*, 107 (2005) 379-386.
- [10] G.K. Mani, J.B.B. Rayappan, A highly selective room temperature ammonia sensor using spray deposited zinc oxide thin film, *Sensors and actuators B: Chemical*, 183 (2013) 459-466.
- [11] J.R. Reddy, G.K. Mani, P. Shankar, J.B. Balaguru Rayappan, Substrate Temperature Effects on Room Temperature Sensing Properties of Nanostructured ZnO Thin Films, *Journal of Nanoscience and Nanotechnology*, 16 (2016) 489-496.
- [12] A.J. Kulandaisamy, J.R. Reddy, P. Srinivasan, K.J. Babu, G.K. Mani, P. Shankar, J.B.B. Rayappan, Room temperature ammonia sensing properties of ZnO thin films grown by spray pyrolysis: Effect of Mg doping, *Journal of Alloys and Compounds*, 688, Part A (2016) 422-429.
- [13] R. Daniel, J. Keckes, I. Matko, M. Burghammer, C. Mitterer, Origins of microstructure and stress gradients in nanocrystalline thin films: The role of growth parameters and self-organization, *Acta materialia*, 61 (2013) 6255-6266.
- [14] P. Carpio, E. Rayón, L. Pawłowski, A. Cattini, R. Benavente, E. Bannier, M.D. Salvador, E. Sánchez, Microstructure and indentation mechanical properties of YSZ nanostructured coatings obtained by suspension plasma spraying, *Surface and Coatings Technology*, 220 (2013) 237-243.
- [15] B.-K. Jang, H. Matsubara, Influence of porosity on hardness and Young's modulus of nanoporous EB-PVD TBCs by nanoindentation, *Materials Letters*, 59 (2005) 3462-3466.
- [16] A. Zeilinger, J. Todt, C. Krywka, M. Müller, W. Ecker, B. Sartory, M. Meindlhumer, M. Stefanelli, R. Daniel, C. Mitterer, J. Keckes, In-situ Observation of Cross-Sectional Microstructural Changes and Stress Distributions in Fracturing TiN Thin Film during Nanoindentation, *Scientific Reports*, 6 (2016) 22670.
- [17] A. Zeilinger, R. Daniel, T. Schöberl, M. Stefanelli, B. Sartory, J. Keckes, C. Mitterer, Resolving depth evolution of microstructure and hardness in sputtered CrN film, *Thin Solid Films*, 581 (2015) 75-79.
- [18] H.F. Pang, G.A. Zhang, Y.L. Tang, Y.Q. Fu, L.P. Wang, X.T. Zu, F. Placido, Substrate-tilt angle effect on structural and optical properties of sputtered ZnO film, *Applied Surface Science*, 259 (2012) 747-753.
- [19] U. Ozgur, D. Hofstetter, H. Morkoc, ZnO Devices and Applications: A Review of Current Status and Future Prospects, *Proceedings of the IEEE*, 98 (2010) 1255-1268.
- [20] W.C. Oliver, G.M. Pharr, An improved technique for determining hardness and elastic modulus using load and displacement sensing indentation experiments, *J. Mater. Res.*, 7 (1992) 1564-1583.
- [21] Q. Tian, H. Liu, Electrophoretic deposition and characterization of nanocomposites and nanoparticles on magnesium substrates, *Nanotechnology*, 26 (2015) 175102.
- [22] Y.-C. Huang, S.-Y. Chang, Substrate effect on mechanical characterizations of aluminum-doped zinc oxide transparent conducting films, *Surface and Coatings Technology*, 204



- (2010) 3147-3153.
- [23] V. Bhardwaj, R. Chowdhury, R. Jayaganthan, Nanomechanical and microstructural characterization of sputter deposited ZnO thin films, *Applied Surface Science*, 389 (2016) 1023-1032.
- [24] R. Saha, W.D. Nix, Effects of the substrate on the determination of thin film mechanical properties by nanoindentation, *Acta Materialia*, 50 (2002) 23-38.
- [25] Y.-M. Hu, S.-S. Li, C.-H. Kuang, T.-C. Han, C.-C. Yu, Post-annealing effect on the room-temperature ferromagnetism in Cu-doped ZnO thin films, *Journal of Applied Physics*, 117 (2015) 17B901.
- [26] S.J. Kang, Y.H. Joung, H.H. Shin, Y.S. Yoon, Effect of substrate temperature on structural, optical and electrical properties of ZnO thin films deposited by pulsed laser deposition, *Journal of Materials Science: Materials in Electronics*, 19 (2008) 1073-1078.
- [27] A. Van der Drift, Evolutionary selection, a principle governing growth orientation in vapour-deposited layers, *Philips Res. Rep.*, 22 (1967) 267-288.
- [28] G.F. Iriarte, J.G. Rodríguez, F. Calle, Synthesis of c-axis oriented AlN thin films on different substrates: A review, *Materials Research Bulletin*, 45 (2010) 1039-1045.
- [29] C. Schuh, T. Nieh, Y. Kawamura, Rate dependence of serrated flow during nanoindentation of a bulk metallic glass, *Journal of Materials Research*, 17 (2002) 1651-1654.
- [30] V. Coleman, J. Bradby, C. Jagadish, P. Munroe, Y. Heo, S. Pearton, D. Norton, M. Inoue, M. Yano, Mechanical properties of ZnO epitaxial layers grown on a-and c-axis sapphire, *Applied Physics Letters*, 86 (2005) 203105.
- [31] R. Navamathavan, K.-K. Kim, D.-K. Hwang, S.-J. Park, J.-H. Hahn, T.G. Lee, G.-S. Kim, A nanoindentation study of the mechanical properties of ZnO thin films on (0001) sapphire, *Applied Surface Science*, 253 (2006) 464-467.
- [32] S.-R. Jian, I.-J. Teng, P.-F. Yang, Y.-S. Lai, J.-M. Lu, J.-G. Chang, S.-P. Ju, Surface Morphological and Nanomechanical Properties of PLD-Derived ZnO Thin Films, *Nanoscale Research Letters*, 3 (2008) 186.
- [33] P. Burnett, D. Rickerby, The scratch adhesion test: an elastic-plastic indentation analysis, *Thin Solid Films*, 157 (1988) 233-254.
- [34] Y.C. Yang, E. Chang, Influence of residual stress on bonding strength and fracture of plasma-sprayed hydroxyapatite coatings on Ti-6Al-4V substrate, *Biomaterials*, 22 (2001) 1827-1836.
- [35] S.O. Kucheyev, J.E. Bradby, J.S. Williams, C. Jagadish, M.V. Swain, Mechanical deformation of single-crystal ZnO, *Applied Physics Letters*, 80 (2002) 956-958.
- [36] R. Wen, L. Wang, X. Wang, G.-H. Yue, Y. Chen, D.-L. Peng, Influence of substrate temperature on mechanical, optical and electrical properties of ZnO: Al films, *Journal of Alloys and Compounds*, 508 (2010) 370-374.
- [37] N. Deyneka-Dupriez, U. Herr, H. Fecht, A. Pfrang, T. Schimmel, B. Reznik, D. Gerthsen, Interfacial adhesion and friction of pyrolytic carbon thin films on silicon substrates, *Journal of Materials Research*, 23 (2008) 2749-2756.
- [38] H. Yoshizawa, J. Israelachvili, Fundamental mechanisms of interfacial friction. 2. Stick-slip friction of spherical and chain molecules, *The Journal of Physical Chemistry*, 97 (1993) 11300-11313.
- [39] Y.B. Ping. Cao, Structural properties of p-type ZnO thin film post-treated by NH<sub>3</sub> plasma method, *Advanced Materials Research*, 1004-1005 (2014) 784-787.
- [40] K. Holmberg, A. Matthews, H. Ronkainen, Coatings tribology—contact mechanisms and surface design, *Tribology International*, 31 (1998) 107-120.
- [41] R. Arnell, The mechanics of the tribology of thin film systems, *Surface and Coatings Technology*, 43 (1990) 674-687.